Coupled Hybrid RANS-LES Research at The University of Manchester

Coupled Hybrid RANS-LES Research at The University of Manchester

A. Revell*, I. Afgan, A. E. A. Ali, M. Camps Santasmasas, T. Craft, A. De Rosis, J. Holgate, D. Laurence, B. E. O. Iyamabo, A. Mole, B. Owen, M. Savoie, A. Skillen, J. Wang, X. Zhang

Multiscale & Mulifidelity Modelling for CFD (M3CFD)
Department of Mechanical, Aerospace & Civil Engineering, The University of Manchester, UK

Abstract

This short communication summarises recent developments and ongoing work on Hybrid RANS-LES Methods (HRLM) at The University of Manchester. Our work is focussed primarily on the development of coupled zonal methods, investigating improvements and novel applications of embedded turbulence simulation via the Synthetic Eddy Method. These activities are centred around the premise that no single modelling methodology will be generally applicable. Not only does this apply to different test cases, but for particular regions of the flow within a single test case. Similarly, when factoring in the computational resources available to the modern-day CFD practitioner, a framework for multifidelity approaches seems pragmatic. The work presented herein is intended primarily as a window through which we outline our current activities, mostly driven by PhD projects, many of which with industrial projects in mind. We also introduce recent developments focused on using the lattice Boltzmann method as part of a coupled Hybrid RANS LES approach.

1 Introduction

Hybrid RANS-LES Methods offer compromise to the accuracy-cost-speed trilemma for simulations at moderate-to-high Reynolds number, and can generally be separated into two distinct classes, 1) Zonal and 2) Non-Zonal (Global). The latter has become more widely used than the former over the past decades, in particular due to the prevalence of Detached Eddy Simulation proposed by Strelets et al. [1], which has received a lot of attention for industrial applications [2]. On the other hand, Zonal approaches such the framework proposed by Deck [3] can offer different advantages. These methods generally employ sub-domains which are then solved individually with a separate set of transport equations. Unlike non-zonal methods, there is a clear and conscious demarcation between mean RANS and transient LES regions. In the transfer to LES regions, instantaneous fluctuations must be generated using information taken from the upstream flow; whereas the mean/modelled turbulent quantities must be recovered from the LES field upon re-entering a RANS region.

At Reynolds numbers of practical engineering interest, the incoming flow will often be turbulent. The generation of turbulent inflow boundary conditions for scale-resolving simulations poses a formidable challenge. A popular solution to this problem is the Synthetic Eddy Method (SEM) of Jarrin et al. [4] whereby Lagrangian spots (or synthetic eddies) are generated to represent

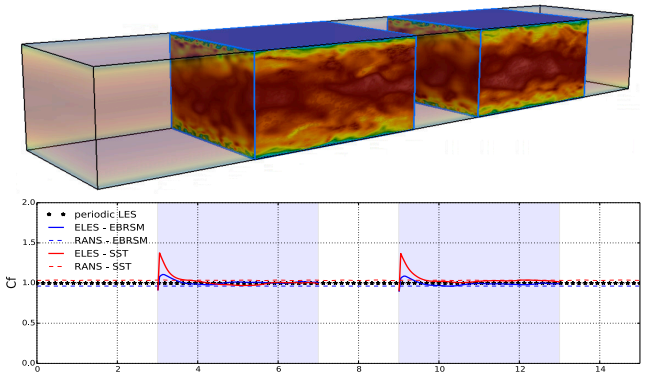

Figure 1: Proof of concept for ELES, **Top**) Two-region nested LES computation coloured by instantaneous velocity. **Btm**) Skin friction coefficient normalised by periodic LES value through the entire channel.

fluctuations, with the intensity and sign set to satisfy prescribed first and second order statistics. In practise, these low-order statistics may be obtained by experiment, theoretical approximation, or as is perhaps the most common, by a separate or precursor RANS study. Embedded LES (ELES) is a natural evolution of this concept, whereby the RANS data generated in one mesh is used directly for the generation of synthetic turbulence and subsequent turbulent simulation in another. An early implementation of ELES is presented by Cokljat et al. [5] who considered a number of internal flow applications and a number of more recent implementations have followed. Notably Li et al. al. [6] validated a two-region ELES solver consisting of a single RANS and implicit LES region and Anupindi & Sandberg [7] implemented an ELES model within OpenFOAM. In a slightly different approach, Vonlanthen et al. [8] introduced a one-way nesting procedure which embeds a highly-resolved LES within a low-resolution LES. For an extensive review of Embedded LES approaches the reader is referred to Holgate et al. [9].

Through work at the University of Manchester, the SEM has evolved in several directions; a divergence-free version was proposed by Poletto et al. [10] and a more efficient formulation was presented by Skillen et al. [11]. More recent work has focused on the code-code coupling aspects, wherein mixed fidelity solvers can be used interchangeably. In particular we have developed ideas based on the Two-Velocity method of Uribe et al. [12], and the consistent Dual-Mesh approach of Xiao and Jenny [13]. These methods solve RANS and LES models simultaneously on separate grids, with added 'drift terms' in the momentum, pressure and turbulent transport equations used to relax the flow statistics towards a consistent solution.

*contact: alistair.revell@manchester.ac.uk

As a final point, it is worth noting that in all the above, zonal methods are enhanced when the upstream prediction of turbulent Reynolds stresses is good. As such there is a rational case for the use and further refinement of advanced turbulence modelling tools in this framework. We have been using the Elliptic Blending model of Manceau and Hanjalić [14] with its demonstrated advantages complex flows [15], as well as models based on the stress-strain lag approach of Revell et al. [16], recently reformulated for elliptic blending [17]. This is highlighted in recent work demonstrating potential for multiple embedded regions, as shown in Figure (1), where faster recovery is observed with the more advanced turbulence model.

2 Recent work with the SEM

As recently demonstrated by Skillen et al. [11], with improved normalisation of the fluctuations on the inlet plane, the Synthetic Eddy Method (SEM) can accomplish a short recovery of the turbulent statistics. However, it remains sensitive to the prescribed variation of the length scale σ to produce realistic turbulence. The length scale of the eddies is generally assigned the following form where C_σ is a scaling factor, discussed further below. $\sigma_i = \min(C_\sigma R_{ii}^{3/2}/\varepsilon\ ,\ \sigma_{\max})$.

Defining the term Eddy Simulation (ES) as applying to both DES and LES methods, and following extensive testing for internal flows, we now consider application to a spatially developing boundary layer case in the fully turbulent regime. A schematic showing how the domain is split between mean and resolved (ES) domain is shown in Figure (2). In this case we use Improved Delayed Detached Eddy Simulations (IDDES) in place of the LES in order to further reduce the computational cost according to Shur et al. [18]. The Reynolds number based on the momentum thickness at the start of the LES region is $Re_\theta = 3040$.

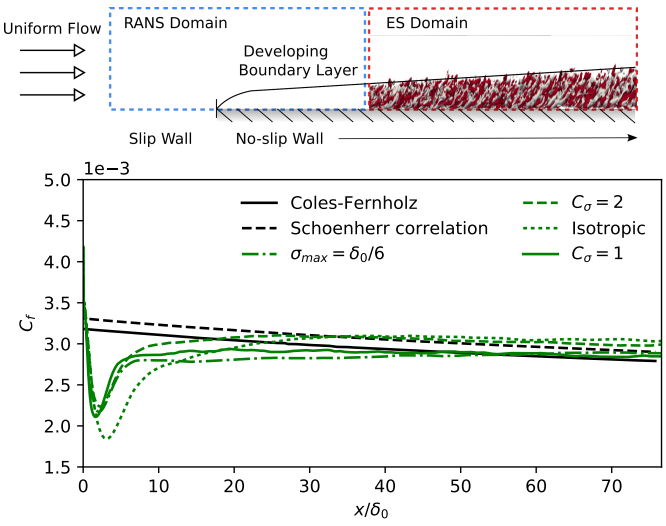

Figure 2: **Top**) Schematic of TBL domain. **Btm**) Downstream recovery of skin friction coefficient C_f.

In order to assess the development length, the evolution of the skin friction coefficient, C_f, along the length of the ES domain is shown in Figure (2). Some sensitivity to imposed length scale variation is observed as also identified in earlier work for internal flows [9], in an attempt to minimise the development length. In this instance increasing the length scale by setting $C_\sigma = 2$ improved the development length. The figure also demonstrates that using an anisotropic length scale definition is a significant improvement over an isotropic definition.

First and second order statistics of the flow at a location downstream of the SEM were also assessed. These are given for a Reynolds number based on the momentum thickness of $Re_\theta = 5200$ and compared to experimental data of DeGraaff & Eaton [19]. Although a degree of log-layer mismatch is present, the close agreement of the statistics suggest that the relationship between the IDDES and the SEM is working.

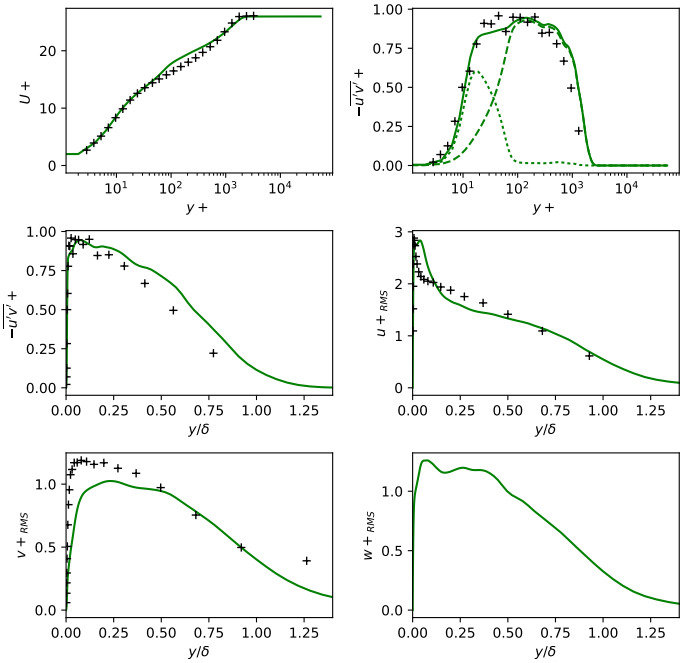

Figure 3: Velocity and Reynolds stress profiles at $Re_\theta = 5200$. *Solid*: Total stress, *Dashed*: Resolved stress, *Dotted*: Modelled stress

As an example of a more complex test for SEM, we consider the case defined by Liu et al. [20] for the superposition of a pair of counter-rotating vortices in a turbulent boundary layer, directly relevant to flow downstream of vortex generators and other flow control devices. Initial work has been performed on a 'Common Flow Down' vortex pair, generated by superimposing Batchelor vortices onto the boundary layer inlet before applying the SEM. Figure (4) shows a visualisation of the flow for this case using Q-iso surfaces.

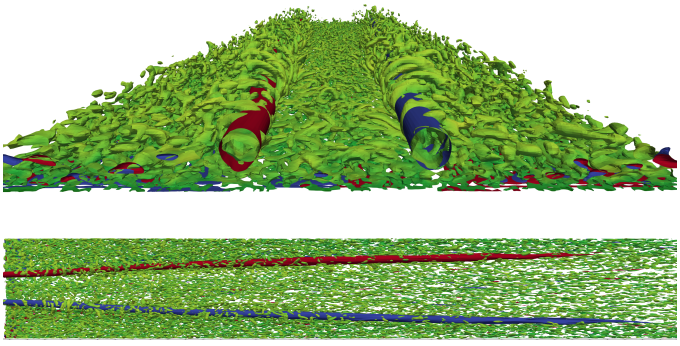

Figure 4: Q-iso surfaces. *Top*: View from inlet, *Bottom*: Side view. *Green*: Instantaneous, *Red and blue*: Mean.

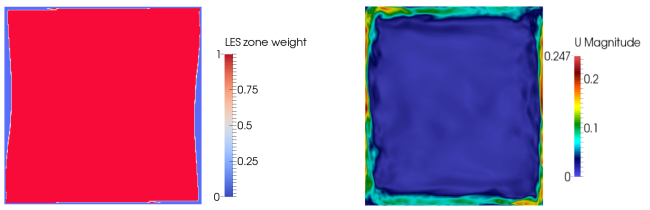

Figure 5: Square Cavity Case. Distribution of the LES zone weight and Instantaneous Velocity

3 Dual Mesh with Heat transfer

In this work, the dual-mesh approach [13] was extended and applied for the first time to natural convection flows, following work by Tunstall et al. [21]. The two cases reported here are a high Rayleigh number differentially heated square cavity flow and the flow in a cylindrical annuli. Detailed descriptions of these test cases can be found in [22] and [23].

In the dual-mesh approach, two separate meshes are produced, tailored to the specific needs of each solver; the RANS grid is refined in the near-wall regions and the LES grid is designed to be under-resolved near the walls of the domain. The two simulations are 'drifted' towards each other using source terms added to the momentum, temperature and turbulence equations of the RANS and the LES. A novel criterion is introduced to predict the locations at which the LES is under-resolved. At these locations, the mean velocity and temperature, total turbulent kinetic energy and total temperature variance (the latter two including resolved and modelled contributions) of the LES solution are corrected towards the corresponding RANS quantities. At remaining locations, the RANS solution is corrected towards the solution of the LES. More details about the formulation of the method can be found in [13] and [21].

A new criterion has been introduced based on the ratio of the turbulence length scales to the grid size; designed to account for the presence of both turbulent and laminar regions within the flow domain. Reasonable results for the square cavity and cylindrical annuli flows were obtained when the new criterion was used. Results for the square cavity are shown in Figure (5) which displays the LES zone weight (σ^L) as well as the instantaneous velocity. This quantity is equal to 0 at locations where RANS drives the LES, and equals unity at all other locations. It can be observed that the new criterion returns a rational variation, with σ^L=0 restricted to the near-wall regions of the boundary layers. This is in contrast with the original formulation of the model and demostrates the criteria's ability to discern near-wall flow from laminarization that occurs in the core of the cavity due to the stable stratification.

With regards to the cylindrical annuli flow, a schematic of the flow geometry is shown in Figure (6). In this figure, the tangential velocity component at a line located at an angle of 60° is also shown and compared to quasi-direct numerical simulation data from [23]. It can be seen that RANS and LES results from the dual-mesh framework (solid lines) offer improved prediction when compared to the RANS and LES results computed alone (dashed lines).

4 Subdomain Wall Function

In addition to the work presented in the previous section, we are developing a modified approach wherein

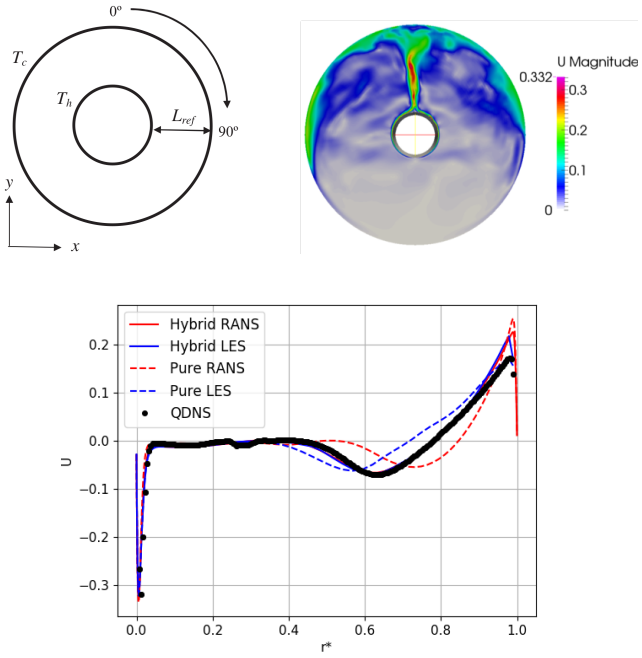

Figure 6: **Top**) Schematic of the cylindrical annuli and Instantaneous Velocity from simulation. **Btm**) Tangential velocity along radius at 60°.

the RANS mesh covers only a narrow near wall region, termed a subdomain wall function (SWF). This method shares much with the previous section and is similar to the wall-modelled LES (WMLES) of Balaras et al. (1996)[24]. As portrayed in Figure (3), the primary domain covers the entire region of the flow field and computes the transport equations of LES. The second domain, termed here the subdomain, overlaps the near-wall area of the coarse LES grid and solves the RANS equations. The two domains are coupled to exchange information between grids. The SWF makes use of ideas of Xiao and Jenny[13] by applying the wall function as a weak volumetric source term in the near-wall LES region beyond the first cell at the wall. This source term corrects the under-resolved near-wall LES fields. In return, the LES grid supplies information to the interface of the RANS grid to complete the boundary conditions of the RANS subdomain. A consistent coupling at the interface is established by computing the partial time average of the instantaneous LES fields. The use of the partial mean differentiates the method from previous WMLES approaches which instead couple instantaneous LES directly to the RANS values.

The partial time-average of LES fields of interest is computed using the exponentially weighed average (EWA), where the averaging time period is sufficiently long to ensure the assumption that the partial time-averaged filtered LES velocity is equivalent to the Reynolds-averaged velocity ($\langle\overline{U_i}\rangle^{EWA} \approx \langle U_i\rangle^{RANS}$). This assumption enables the calculation of the resolved fluctuations about the EWA of the filtered velocity as $u_i^{''} = \overline{U_i} - \langle\overline{U_i}\rangle^{EWA}$. The LES stress tensor is determined as the summation of the resolved and modelled stresses about the EWA of the filtered velocity $\tau_{ij} = u_i^{''} u_j^{''} + \tau_{ij}^r$. Hence, the LES stress tensor is assumed to be equivalent to the RANS stress tensor as $\langle\tau_{ij}\rangle^{EWA} \approx \langle u_i u_j\rangle^{RANS}$.

The momentum transport equation for the LES domain is defined as:

$$\frac{\partial\overline{U_i}}{\partial t} + \frac{\partial\overline{U_i}\,\overline{U_j}}{\partial x_j} = -\frac{\partial P}{\partial x_i} + 2\nu\frac{\partial}{\partial x_j}\overline{S_{ij}} - \frac{\partial\tau_{ij}^r}{\partial x_j} + Q_i, \quad (1)$$

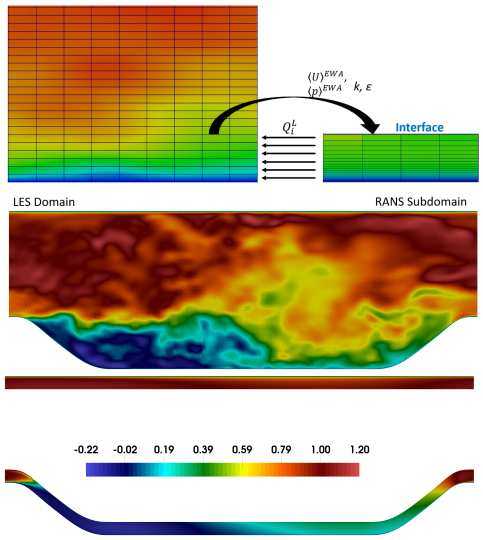

Figure 7: **Top**) Schematic of the subdomain wall function for LES. **Btm**) Contours of the LES and RANS domains predicted by the subdomain wall function

where Q_i is the drift term which is defined as:

$$Q_i = (1-\sigma^L)\left[\frac{\langle U_i\rangle^{RANS} - \langle\overline{U_i}\rangle^{EWA}}{\gamma_{l1}} + \frac{G_i}{\gamma_{l2}}\right]. \qquad (2)$$

The variable σ^L is the zoning parameter that determines the areas of the LES grid that are under-resolved. The drift term is only active in the area of the LES grid that overlaps the RANS subdomain. The left term in the square bracket of the drift term relaxes the partial mean filtered LES velocity towards the velocity field of the RANS subdomain. Also, the right term G_i rescales the trace of the LES stress tensor towards the RANS turbulent kinetic energy. The RANS subdomain sends information to the LES grid to enable the computation of the drift term. On the other hand, the subdomain receives partial time-averaged LES fields of velocity and pressure at the interface to complete the boundary conditions of the RANS. This work makes use of eddy viscosity models in the subdomain, and so the interface receives the trace of the LES stress tensor ($k^{RANS} = 0.5\langle\tau_{ij}\rangle^{EWA}$) and the LES dissipation rate ($\epsilon^{LES} = 2\nu\overline{S_{ij}S_{ij}} - \tau_{ij}^{SGS}\overline{S_{ij}}$).

The performance of the new method is applied to the $Re_\tau = 10,595$ flow through periodic hills as shown in Figure (7), which displays contour plots for both LES and RANS regions. Present results are then compared on Figure (8) with wall-resolved LES of Breuer et al. (2009)[25] which employed a mesh of 13M cells; noting that the present mesh as less than 0.6M cells, a factor of 20 less. For reference results for LES using the same coarse grid without the SWF are also included. The benefit of the wall function is clear in the near-wall velocity field of the LES towards the RANS, and overall SWF results are in excellent agreement with the reference data.

5 Turbulence with LBM

Nowadays, the lattice Boltzmann method (LBM) is a consolidated approach to simulate fluid flows. Its popularity at least in part stems from the intrinsic simplicity of the Bhatnagar-Gross-Krook (BGK) collision operator [27], where all the populations are forced to relax towards a discrete equilibrium state derived by applying a Gauss-Hermite quadrature to the continuous

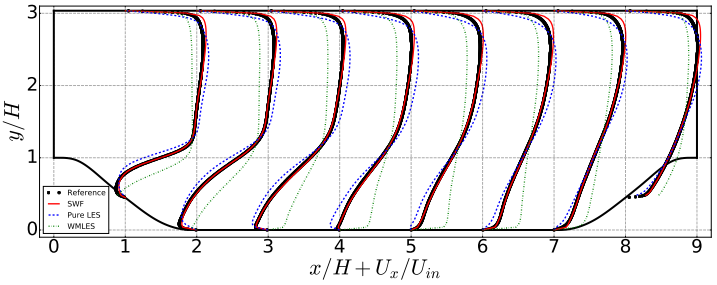

Figure 8: Profiles of the mean streamwise velocity in the LES domain. Red line: SWF; Green line: Pure LES; Blue line: WMLES; Black markers: reference data

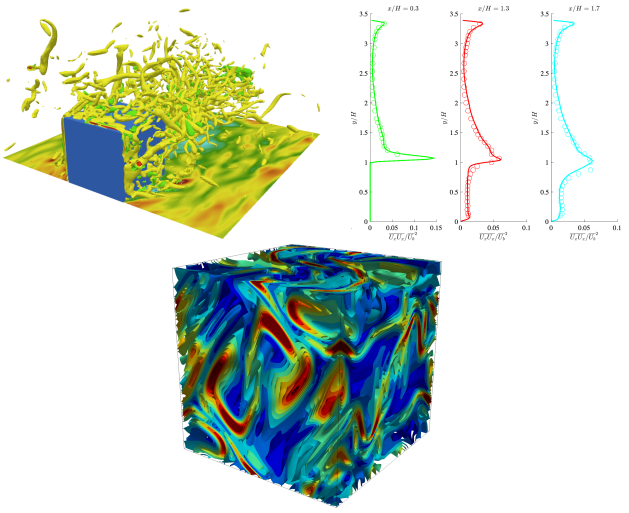

Figure 9: **Top**) LUMA validation for turbulent flow over cube array of [26], Q-criterion and profiles of streamwise normal Reynolds stress. **Btm**) Simulation of a magneto-hydrodynamic vortex in three dimensions for Re = 570.

Maxwellian distribution. However, the BGK model is well known to be prone to numerical instability in the low-viscosity regime, thus becoming unsuitable for the prediction of turbulent flows. To cope with this problem, a family of collision models based on the relaxation of central moments (CMs) was introduced in 2006 [28]. Here, the collision process shows pyramidal hierarchical topology, where the post-collision state of CMs is constructed starting from the lowest order, and then proceeding in ascending sequence, hence the name *cascaded* lattice Boltzmann method. It has been demonstrated to outperform both BGK and multiple-relaxation-time [29] LBM in terms of stability (the latter based on absolute moments).

More recently, we approached central moments from a different viewpoint. Given a certain lattice, our methodology consists of building a transformation matrix allowing us to move from the space of populations to the one of central moments and vice-versa. The resultant algorithm loses the above-mentioned pyramidal cascaded structure and, as a consequence, it can be interpreted as a *non-cascaded* way to apply the collision step in CMs space [30, 31]. Interestingly, it is also shown that the present method recovers the behaviour of the cascaded LBM while allowing the derivation of forcing terms in an a systematic and straightforward manner. This was thoroughly demonstrated by successfully recovering different sets of governing equations with this approach, hence allowing the simulation of a rich variety of physics

problems such as magnetohydrodynamics [32] and multicomponent flows [33] among others. As an example, Figure (9) shows an instantaneous snapshot from a turbulent magnetohydrodynamics case.

The group has recently developed a lattice Boltzmann (LB) code primarily for the purpose of testing new approaches. LUMA (LBM at The University of Manchester) [34] offers grid refinement, turbulence and fluid-structure interaction, and a GPU version is now in development based on our earlier work [35]. Validation results for turbulent flow are displayed in Figure (9) for the periodic cube array case of [26]. Ongoing work is in progress to further develop our LBM capabilities in the context of hybrid RANS LES methods.

6 A Dual-Solver using LBM

A natural evolution of the dual mesh approach is to use different codes for each region. In this work, focused on developing fast prediction for turbulent flow around urban geometries, the solver in the region of interest is a lattice Boltzmann (LB) solver based on [34] running on GPUs. Since the LB region is a small volume of the domain the hybrid model overcomes the mesh and memory related drawbacks of using GPU accelerated LB, while maintaining its inherent speed and accuracy. The solver for the remainder of the domain is a finite volume RANS solver running on CPU, which takes advantage of the mesh flexibility and lower memory consumption of the NS algorithm. Moreover, the RANS-LBLES model exploits the availability of heterogeneous CPU/GPU hardware on consumer devices.

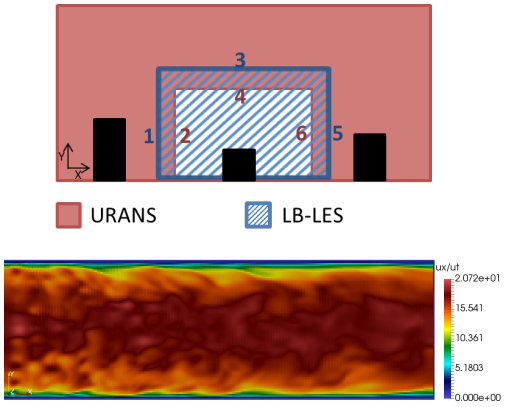

Figure 10: **Top**) Dual solver concept **Btm**) Streamwise instantaneous velocity on vertical section of a channel flow using SEM with LBM.

The method uses two fully-coupled sub-domains as shown in Figure (10), wherein the LBLES and the RANS regions exchange required information at overlapping interfaces, marked with numbers in Figure (10). Odd numbers denote the LBLES boundaries that receive data from the RANS solver, while the even numbers denote RANS boundaries that receive data from the LBLES solver. The volume between them is the overlap region, which is part of both sub-domains. The external boundaries (boundaries 1, 3 and 5) incorporate the Synthetic Eddy Method (SEM) to generate the instantaneous velocity as needed by the LES. The two subdomains are coupled using the parallel explicit algorithm in the preCICE libraries [36]. In this framework it is noted that eventually unsteady mean flow i.e. URANS could be coupled with LES in the same way.

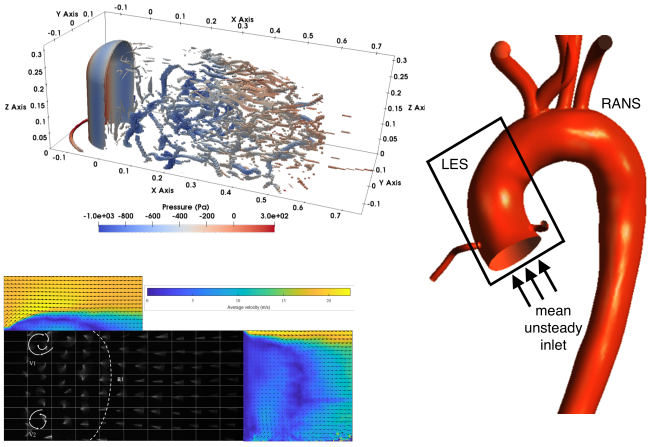

Figure 11: Ongoing work: **Top**) Isosurface of Q-criterion for flow around GSM, **Btm**) Experimental validation case for truck aerodynamics, Embedded simulation for cardiovascular flow.

The SEM inlet boundary has been implemented within a lattice Boltzmann solver for the first time, and tested fo a channel flow at $Re_\tau = 180$, where the domain is discretised using a uniform Cartesian grid with $y^+ = 4$. Figure (10) displays the streamwise components of the instantaneous velocity u_x/u_τ.

7 Conclusions and Ongoing work

This communication has provided a brief overview of recent and ongoing activities in our group at The University of Manchester in the context of Hybrid RANS LES methods; the interested reader is invited to contact us where more details are desired. These activities underpin our primary objective to develop a set of computational tools which enable fast and efficient coupling between different levels of modelling fidelity. The resulting series of coupled Hybrid RANS LES methods are applicable across a range of applications. Furthermore, we have demonstrated the potential for combining lattice Boltzmann method in this framework, particularly given its inherent scalability on GPU processors.

Work in our group is also in progress on the more applied side, in particular testing their potential for application to complex configurations which cover a range of lengthscales. Examples include the assessment of wind turbines on environmental landscapes [37], assessment of individual buildings in context of city-scale flows, application to ground vehicles aerodynamics [38, 39] and cardiovascular flow in and around the heart [40, 41]. One ongoing study is motivated by noise levels in road vehicles, wherein we will apply the dual solver approach in section 6 to a generic side mirror (GSM) model [42], consisting of a quarter sphere mounted on a half cylinder. Thus far, work has focused on using Delayed Detached Eddy Simulation (DDES) but will soon incorporate LBM also; initial results are displayed in Figure (11). Other ongoing work will apply these methods to truck 0 in tandem, with an experimental campaign. Finally, we are also starting to apply coupled HRLM to cardiovascular flows as proposed in Figure (11).

Acknowledgment

We acknowledge support from the UK Turbulence Consortium (EPSRC Grant EP/G069581/1) and The UK

Consortium on Mesoscale Engineering Sciences (Grant No. EP/L00030X/1), both of which provided computational access to ARCHER, UK. The authors also acknowledge assistance from IT Services and the use of the Computational Shared Facility at The University of Manchester.

References

[1] M. Strelets, "Detached eddy simulation of massively separated flows," in *39th AIAA Aero. sciences meet*, p. 879, 2001.

[2] W. Haase, M. Braza, and A. Revell, *DESider–A European Effort on Hybrid RANS-LES Modelling: Results of the European-Union Funded Project, 2004-2007*, vol. 103. Springer Science & Business Media, 2009.

[3] S. Deck, "Zonal-detached-eddy simulation of the flow around a high-lift configuration," *AIAA journal*, vol. 43, no. 11, pp. 2372–2384, 2005.

[4] N. Jarrin, S. Benhamadouche, D. Laurence, and R. Prosser, "A synthetic-eddy-method for generating inflow conditions for large-eddy simulations," *International Journal of Heat and Fluid Flow*, vol. 27, no. 4, pp. 585–593, 2006.

[5] D. Cokljat, D. Caridi, S. Sheffield, G. Link, F. Menter, and A. G. Gmbh, "Embedded LES Methodology for General-Purpose CFD Solvers," *6th International Symposium on Turbulence and Shear Flow Phenomena*, pp. 1191 – 1196, 2009.

[6] Z. Li, H. Chen, and Y. Zhang, "Validation of a Window-Embedded RANS/LES Method Based on Synthetic Turbulence," *54th AIAA Aero. Sciences Meet.*, pp. 1–8, jan 2016.

[7] K. Anupindi and R. Sandberg, "Implementation and Evaluation of an Embedded LES-RANS Solver," *Flow, Turbulence and Combustion*, 2016.

[8] M. Vonlanthen, J. Allegrini, and J. Carmeliet, "Assessment of a one-way nesting procedure for obstacle resolved large eddy simulation of the ABL," *Computers & Fluids*, vol. 140, pp. 136–147, nov 2016.

[9] J. Holgate, A. Skillen, T. Craft, and A. Revell, "A review of embedded large eddy simulation for internal flows," *Archives of Comp. Methods in Engineering*, vol. 5, pp. 1–18, 2018.

[10] R. Poletto, T. Craft, and A. Revell, "A New Divergence Free Synthetic Eddy Method for the Reproduction of Inlet Flow Conditions for LES," *Flow, Turbulence and Combustion*, vol. 91, pp. 519–539, jul 2013.

[11] A. Skillen, A. Revell, and T. Craft, "Accuracy and efficiency improvements in synthetic eddy methods.," *Int. J. of Heat and Fluid Flow*, vol. 62, pp. 386–394, 2016.

[12] J. Uribe, A. Revell, and C. Moulinec, "Computation of flow in a 3d diffuser using a two-velocity field hybrid rans/les," in *Turbulence and Interactions*, pp. 385–391, Springer, 2010.

[13] H. Xiao and P. Jenny, "A consistent dual-mesh framework for hybrid LES/RANS modeling," *Journal of Computational Physics*, vol. 231, pp. 1848–1865, feb 2012.

[14] R. Manceau and K. Hanjalić, "Elliptic blending model: A new near-wall reynolds-stress turbulence closure," *Physics of Fluids*, vol. 14, no. 2, pp. 744–754, 2002.

[15] F. Billard, A. Revell, and T. Craft, "Application of recently developed elliptic blending based models to separated flows," *International Journal of Heat and Fluid Flow*, vol. 35, pp. 141–151, 2012.

[16] A. J. Revell, T. J. Craft, and D. R. Laurence, "Turbulence modelling of unsteady turbulent flows using the stress strain lag model," *Flow, Turbulence and Combustion*, vol. 86, no. 1, pp. 129–151, 2011.

[17] S. Lardeau and F. Billard, "Development of an elliptic-blending lag model for industrial applications," in *54th AIAA Aerospace Sciences Meeting*, p. 1600, 2016.

[18] M. L. Shur, P. R. Spalart, M. K. Strelets, and A. K. Travin, "A hybrid rans-les approach with delayed-des and wall-modelled les capabilities," *International Journal of Heat and Fluid Flow*, vol. 29, no. 6, pp. 1638–1649, 2008.

[19] D. DeGraaf and J. Eaton, "Reynolds number scaling of the flat-plate turbulent boundary layer," *Journal of Fluid Mechanics*, vol. 422, pp. 319–346, 2000.

[20] J. Liu, U. Piomelli, and P. R. Spalart, "Interaction between a spatially growing turbulent boundary layer and embedded streamwise vortices," *Journal of Fluid Mechanics*, vol. 326, pp. 151–179, 1996.

[21] R. Tunstall, *CFD and turbulence modelling for Nuclear Plant Thermal hydraulics systems*. PhD thesis, University of Manchester, 2016.

[22] F. Sebilleau, R. Issaa, S. Lardeau, and S. Walker, "Direct Numerical Simulation of an air-filled differentially heated square cavity with Rayleigh numbers up to 1011," *Int. J. of Heat and Mass Transfer*, pp. 297–319, 2018.

[23] Y. Addad, I. Zaidi, and D. Laurence, "Quasi-DNS of natural convection flow in a cylindrical annuli with an optimal polyhedral mesh refinement," *Computers and Fluids*, vol. 118, p. 44âĂŞ52, 2015.

[24] E. Balaras, C. Benocci, and U. Piomelli, "Two-layer approximate boundary conditions for large-eddy simulations," *AIAA Journal*, vol. 34, pp. 1111–1119, 1996.

[25] M. Breuer, N. Peller, C. Rapp, and M. Manhart, "Flow over periodic hills - Numerical and experimental study in a wide range of Reynolds numbers," *Computers and Fluids*, vol. 38, no. 2, pp. 433–457, 2009.

[26] E. Meinders and K. Hanjalić, "Vortex structure and heat transfer in turbulent flow over a wall-mounted matrix of cubes," *International Journal of Heat and fluid flow*, vol. 20, no. 3, pp. 255–267, 1999.

[27] P. Bhatnagar, E. Gross, and M. Krook, "A model for collision processes in gases. I. small amplitude processes in charged and neutral one-component systems," *Phys. Rev.*, vol. 94, no. 3, p. 511, 1954.

[28] M. Geier, A. Greiner, and J. Korvink, "Cascaded digital lattice Boltzmann automata for high Reynolds number flow," *Phys. Rev. E*, vol. 73, no. 6, p. 066705, 2006.

[29] D. d'Humières, I. Ginzburg, M. Krafczyk, P. Lallemant, and L.-S. Luo, "Multiple-relaxation-time lattice Boltzmann models in three dimensions," *Phil. Trans. R. Soc. A*, vol. 360, pp. 437–451, 2002.

[30] A. De Rosis, "Nonorthogonal central-moments-based lattice boltzmann scheme in three dimensions," *Phys. Rev. E*, vol. 95, no. 1, p. 013310, 2017.

[31] A. De Rosis and K. H. Luo, "Role of higher-order hermite polynomials in the central-moments-based lattice boltzmann framework," *Phys. Rev. E*, vol. 99, no. 1, p. 013301, 2019.

[32] A. De Rosis, E. Lévêque, and R. Chahine, "Advanced lattice boltzmann scheme for high-reynolds-number magneto-hydrodynamic flows," *J. Turbul.*, pp. 446–462, 2018.

[33] S. Saito, A. De Rosis, A. Festuccia, A. Kaneko, Y. Abe, and K. Koyama, "Color-gradient lattice boltzmann model with nonorthogonal central moments: Hydrodynamic melt-jet breakup simulations," *Phys. Rev. E*, vol. 98, 2018.

[34] A. R. G. Harwood, J. O'Connor, J. S. M. noz, M. C. Santasmasas, and A. J. Revell, "LUMA: A many-core, Fluid-Structure Interaction solver based on the Lattice-Boltzmann Method," *SoftwareX*, vol. 7, pp. 88–94, 2018.

[35] M. J. Mawson and A. J. Revell, "Memory transfer optimization for a lattice boltzmann solver on kepler architecture nvidia gpus," *Computer Physics Communications*, vol. 185, no. 10, pp. 2566–2574, 2014.

[36] H. J. Bungartz, F. Lindner, B. Gatzhammer, M. Mehl, K. Scheufele, A. Shukaev, and B. Uekermann, "pre-CICE A fully parallel library for multi-physics surface coupling.," *Computers and Fluids*, vol. 141, pp. 250–258, 2016.

[37] S. Hewitt, L. Margetts, and A. Revell, "Building a digital wind farm," *Archives of Computational Methods in Engineering*, vol. 25, no. 4, pp. 879–899, 2018.

[38] N. Ashton and A. Revell, "Key factors in the use of dde for the flow around a simplified car," *International Journal of Heat and Fluid Flow*, vol. 54, pp. 236–249, 2015.

[39] N. Ashton, A. West, S. Lardeau, and A. Revell, "Assessment of rans and des methods for realistic automotive models," *Computers & Fluids*, vol. 128, pp. 1–15, 2016.

[40] M. G. Al-Azawy, A. Turan, and A. Revell, "Assessment of turbulence models for pulsatile flow inside a heart pump," *Computer methods in biomechanics and biomedical engineering*, vol. 19, no. 3, pp. 271–285, 2016.

[41] B. Owen, C. Lowe, N. Ashton, P. Mandal, S. Rogers, W. Wein, C. McCollum, and A. Revell, "Computational hemodynamics of abdominal aortic aneurysms: three-dimensional ultrasound versus computed tomography," *Proceedings of the Institution of Mechanical Engineers, Part H: Journal of Engineering in Medicine*, vol. 230, no. 3, pp. 201–210, 2016.

[42] R. Siegert, V. Schwarz, and J. Reichenberger, "Numerical Simulation of aeroacustic sound generated by generic bodies placed on a plate: Part II - Prediction of Radiated Sound Pressure," *5th AIAA/CEAS Aeroacoustics Conference and Exhibit*, no. May, 1999.